R. & M. No. 3076
(19,319)
A.R.C. Technical Report

MINISTRY OF SUPPLY

AERONAUTICAL RESEARCH COUNCIL
REPORTS AND MEMORANDA

The Wave Drag of Non-Lifting Combinations of Thin Wings and 'Non-Slender' Bodies

By

L. M. SHEPPARD

LONDON: HER MAJESTY'S STATIONERY OFFICE
1958
PRICE 6*s.* 6*d.* NET

The Wave Drag of Non-Lifting Combinations of Thin Wings and 'Non-Slender' Bodies

By

L. M. SHEPPARD*

COMMUNICATED BY THE DIRECTOR-GENERAL OF SCIENTIFIC RESEARCH (AIR)
MINISTRY OF SUPPLY

Reports and Memoranda No. 3076†
March, 1957

Summary.—The methods of wave-drag estimation known as the area rule and transfer rule are restricted to non-lifting combinations of thin wings and slender bodies. The Lomax-Heaslet multipole method is applicable to configurations with 'non-slender' fuselages, represented by an axial distribution of multipoles. However, it is not entirely satisfactory and an alternative multipole method is presented here. This is based upon the assumption, fundamental to the area rule and the transfer rule, that the effect on the wave drag of the interference velocity potential, due to the interaction between the exposed wing and the fuselage, is negligible. An investigation of the validity of this fundamental assumption based on existing theoretical and experimental results, is given. The application of the multipole method to fuselage design for low combination wave drag is discussed with special reference to an elliptic wing-body combination.

1. *Introduction.*—Investigations of wing-body wave drag, under non-lifting conditions, have been made by a number of authors[1 to 6] within the restrictions of the linearised theory, which assumes small perturbation velocities. The specification of non-lifting conditions implies that the wing-body combination has two planes of symmetry and that it can be represented by a distribution of sources over its surface. For such configurations, linearised-theory methods have been developed for estimating wave drag and for shaping the fuselage or main body so that the total combination wave drag is a minimum. Three useful methods known as the area rule[1], the transfer rule[2] and the moment of area rule[3] have been derived using the assumption that the effect on the wave drag of the interference velocity potential, due to the interaction between the body and the exposed wing, is negligible. Since these three methods utilise the same assumption it can be shown[4] that they are equivalent.

Applications of the area rule[1] and its variants[2, 3] are restricted to combinations of thin wings and slender bodies only: thus an extension of the area rule[1] to combinations incorporating 'non-slender' fuselages with more complicated cross-sectional shapes may be desirable. Such an extension has been presented by Lomax and Heaslet[5] who consider fuselages that can be represented by smooth axial distributions of multipole singularities. However, this extension by Lomax and Heaslet[5] is not entirely satisfactory for two reasons: firstly, their comparisons between results for the wave drag of modified and unmodified combinations are not necessarily valid because the same assumption is not made in the two cases; secondly, it may be questioned whether their fuselage designs are optima for the given conditions. It is the purpose of the

* Attached scientist from the Weapons Research Establishment, Salisbury, South Australia.
† R.A.E. Tech. Note Aero. 2496, received 5th June, 1957.

present paper to examine the Lomax-Heaslet multipole method[5] in more detail and to present an alternative method. No attempt is made to apply the exact linearised-theory method of Nielsen[6] which is applicable to quasi-cylindrical fuselages of almost circular cross-section only and is very complex.

In section 2 a brief summary of the area rule[1] and its variants[2,3] are given. In section 3 the extension of the area rule[1] to combinations with ' non-slender ' fuselages is examined, the neglect of the effect of the interference velocity potential being emphasised. For three particular configurations, the range of validity of this assumption is investigated in section 4. In section 5 the illustrative example of an elliptic wing and body combination, considered by Lomax and Heaslet[5], is presented and some theoretical results are compared with existing experimental results. Finally, in section 6, the conclusions of this paper are given.

2. *Configurations with Slender Fuselages.*—The wing-body combinations treated in this section are assumed to have the local surface slope, in the free-stream direction, small everywhere, so that the perturbation velocities are small and the linearised theory is applicable. Since the fuselage is slender, the essential requirement at a Mach number M is that $R\sqrt{(M^2-1)}/l$ be small, where R is a fuselage radius in any cross-section and l is the fuselage length. In addition, the local fuselage radius of curvature, in any meridian section, must always be large compared with the length l.

2.1. *Methods of Estimating Wave Drag.*—For configurations with smooth slender fuselages the area rule[1], transfer rule[2] and moment of area rule[3] methods can be used to estimate the total wave drag. The area rule[1] expresses the wave drag D as a triple integral of the form

$$D = \frac{1}{2\pi}\int_0^{2\pi} d\theta \left[-\frac{q}{2\pi}\int\int S''(x_1, \theta, M)S''(x_2, \theta, M) \log |x_1 - x_2|\, dx_1\, dx_2 \right], \qquad (1)$$

where q is the kinetic pressure $\frac{1}{2}\rho_0 U_0^2$,

ρ_0, U_0 are the free-stream density and velocity respectively,

$S(x, \theta, M)$ defines an elemental area distribution,

$S''(x, \theta, M)$ denotes $\dfrac{\partial^2 S(x, \theta, M)}{\partial x^2}$

and the double integral containing $S(x, \theta, M)$ includes all values of x for which $S(x, \theta, M)$ is defined. It is assumed that $S'(x, \theta, M)$ is continuous everywhere (i.e., $S(x, \theta, M)$ is ' smooth ')*. For a thin wing lying in the plane $z = 0$ (*see* Fig. 1), an elemental wing area distribution[4] is defined by

$$S_W(x, \theta, M) = \int_{T\neq 0} T(x + By_1 \cos\theta\, , y_1)\, dy_1\, , \qquad (2)$$

where $T(x, y)$ denotes the wing thickness at the point (x, y),

$B = \sqrt{(M^2-1)}$, M being the free-stream Mach number,

and θ is a cylindrical polar co-ordinate (*see* Fig. 1). The general expression for an elemental wing area distribution is similar to equation (2) and has been given elsewhere[4]. The complete elemental area distribution is now given to a sufficient approximation by $S(x, \theta, M) = S(x) + S_W(x, \theta, M)$, where $S(x)$ is the fuselage cross-sectional area distribution.

* Lock's investigation[7] of rectangular wings indicates that this smoothness condition is not necessary for wings. Hence the fuselage only need be ' smooth '; this less restrictive condition will not be used here.

If the isolated exposed* wing wave drag is written in the form

$$D_W = \frac{1}{2\pi}\int_0^{2\pi} D\{S_W(x, \theta, M)\}\, d\theta ,$$

where

$$D\{S_W(x, \theta, M)\} = -\frac{q}{2\pi}\int\int S_W''(x_1, \theta, M) S_W''(x_2, \theta, M) \log |x_1 - x_2|\, dx_1\, dx_2 \quad .. \quad .. \quad (3)$$

denotes the wave drag associated with the area distribution $S_W(x, \theta, M)$, then equation (1) becomes the transfer rule[2] and the wave drag can be written as

$$D = D_W + D\{S + A\} - D\{A\} , \quad .. \quad .. \quad .. \quad .. \quad .. \quad (4)$$

where $D\{A\}$, $D\{S + A\}$ denote the wave drags associated with the area distributions $A(x)$, $S(x) + A(x)$ respectively. $A(x)$ is called the transferred wing area distribution[2,4] and may be defined by

$$A(x) = \frac{1}{2\pi}\int_0^{2\pi} S_W(x, \theta, M)\, d\theta , \quad .. \quad .. \quad .. \quad .. \quad .. \quad .. \quad .. \quad (5)$$

so that $A(x)$ is seen to be equal to the mean wing elemental area distribution[1, 4]. Since $S_W'(x, \theta, M)$ is assumed to be continuous everywhere it follows that $A'(x)$ is continuous everywhere.

The transfer rule, equation (4), can be written in the form

$$D = D_W + D_{WB} + D_B$$

where D_{WB} is the interference wave drag and $D_B = D\{S\}$ is the isolated body wave drag. It follows that the interference wave drag is

$$D_{WB} = D\{S + A\} - D\{S\} - D\{A\} . \quad .. \quad .. \quad .. \quad .. \quad .. \quad .. \quad (6a)$$

This result can be written as

$$D_{WB} = -\frac{q}{\pi}\int\int S''(x_1)A''(x_2) \log |x_1 - x_2|\, dx_1\, dx_2 . \quad .. \quad .. \quad .. \quad .. \quad (6b)$$

The moment of area rule[3, 4] expresses the wave drag in a series of ascending powers of $B^2 = M^2 - 1$ beginning with the slender term which is independent of B. Because of the complexity of the result only the first two terms are normally considered. Thus the moment of area rule is applicable to configurations which are described here as ' not-so-slender '. For this reason the method will not be discussed further and attention will be concentrated upon methods, such as the area rule[1] and the transfer rule[2], which are applicable to any configuration.

2.2. *Fuselage Design for Low Wave Drag.*—The design of the fuselage so that the total combination wave drag is a minimum, subject to certain conditions, requires the use of equation (4). In equation (4), the only term dependent upon the fuselage is $D\{S + A\}$ and so this term is required to be minimised. This can be done using the optimum area distributions presented by Eminton[8] and an optimum fuselage cross-sectional area distribution $S(x)$ obtained. Since the fuselage is slender the cross-sectional shape is arbitrary and, therefore, an axisymmetric fuselage shape is theoretically as good as any other shape.

* Here a distinction is made between the expressions exposed wing and net wing. The exposed wing is that part of the gross wing actually outside the fuselage; the net wing is formed by placing the exposed wing panels together. In section 4.1 the net wing is introduced.

3. *Configurations with Non-slender Fuselages.*—Wing-body combinations with non-slender fuselages are examined in this section. The term ' non-slender ' is applied to fuselages which are such that, at a Mach number M, $R\sqrt{(M^2-1)}/l$ is not small everywhere, R being a fuselage radius in a cross-section and l the fuselage length. Non-slender fuselages could be quasi-cylinders, including quasi-cylinders of almost circular cross-section, and bodies with cross-sections of ' figure-of-8 ' type so that, in meridian sections, the profile varies from apparently slender to apparently quasi-cylindrical.

In section 3.1.1 some properties of axial multipole distributions are summarised. Also, the representation of fuselages by axial distributions of multipoles as well as the replacement of wing source sheets by equivalent multipoles are discussed. Next, the fundamental result, giving the wave drag of a wing and non-slender body combination, is derived. In section 3.1.2 this important result is used to give a method of fuselage design for low combination wave drag. Lastly, in section 3.2, the present multipole method is compared with the Lomax-Heaslet multipole method.

3.1. *A Multipole Method.*—3.1.1. *Estimation of wave drag.*—Consider an axial distribution of multipoles and let them be defined by the strength functions $F_n(x)$ ($n = 0, 2, 4, \ldots$), which are believed to be new and are introduced in the Appendix, equation (A.5). The wave drag associated with these multipoles is, from equation (A.6),

$$D = D\{F_0\} + \tfrac{1}{2}\sum_{n=1}^{\infty} D\{F_{2n}\}, \qquad \ldots \quad (7)$$

which is an infinite series in general. The wave drag $D\{F_n\}$ ($n = 0, 2, 4, \ldots$) is given by equation (3). For a given configuration the strength functions $F_n(x)$ will vary with free-stream Mach number M. When $M = 1$ only the strength function $F_0(x)$ is non-zero. However, at free-stream Mach numbers greater than unity the strengths of the higher order multipoles become increasingly important (thus the number of terms required in equation (7) to represent adequately the wave-drag increase with Mach number). This means that the complexity of any wave-drag calculations will increase rapidly with increasing Mach number.

Singularity representations for the non-slender fuselages considered in this paper are assumed to consist of smooth axial distributions of multipole singularities. If the multipole strength functions are known equations (A.3), (A.4) in the Appendix enable the fuselage, which is a stream surface, to be calculated[5]. However, the inverse problem of determining the multipole strength functions associated with a given body shape is more difficult and the general case has not been solved since it requires the solution of the integral equations (A.3), (A.4). For the special case of slender fuselages $F_{0B}(x) = S(x)$, the body cross-sectional area distribution, and $F_{nB}(x) \simeq 0$, $n > 0$. Moreover, if the fuselage is axisymmetric $F_{nB}(x) = 0$, $n > 0$ and the singularity representation consists of only axial sources, whose strength can be found by superposing a number of Ferrari's conical-body solutions[9], for example. For many non-slender fuselages it may be sufficient to use only a source, $F_{0B}(x)$, and quadrupole, $F_{2B}(x)$, representation, provided that the fuselage is not a quasi-cylinder of almost circular cross-section; in this case the multipole strength functions can be found directly by using the method of Nielsen[6].

Although the wing singularity representation may be a planar distribution of sources, the special representation used here is in terms of equivalent axial distributions of multipoles. Lomax and Heaslet[5] have derived an axial distribution of multipoles which is equivalent to the sources in the sense that the same perturbation velocities at infinity are associated with the equivalent multipoles and the sources, i.e., the same wave drag is associated with the sources and the equivalent multipoles. These equivalent wing multipoles have strength functions $F_{nW}(x)$ defined by

$$\left.\begin{aligned} F_{0W}(x) &= \frac{1}{2\pi}\int_0^{2\pi} S_W(x, \theta, M)\, d\theta \\ F_{nW}(x) &= \frac{1}{\pi}\int_0^{2\pi} S_W(x, \theta, M)\cos n\theta\, d\theta \qquad (n > 0) \end{aligned}\right\} \quad \ldots \quad (8)$$

or, alternatively,

$$\left.\begin{aligned} F_{0W}(x) &= \frac{1}{\pi}\iint \frac{T(x_1, y_1)\, dx_1 dy_1}{\sqrt{\{B^2 y_1^{\,2} - (x - x_1)^2\}}} \\ F_{nW}(x) &= \frac{2}{\pi}\iint \frac{T(x_1, y_1) \cos\left[n \cos^{-1}\left(\frac{x_1 - x}{By_1}\right)\right] dx_1\, dy_1}{\sqrt{\{B^2 y_1^{\,2} - (x - x_1)^2\}}} \qquad (n > 0) \end{aligned}\right\}. \tag{9}$$

In equation (8), $S_W(x, \theta, M)$ denotes an elemental wing area distribution (equation (2)). Since $S_W(x, \theta, M)$ varies with Mach number, it follows that $F_{n\,W}(x)$ will vary with Mach number also. In equation (9), $T(x, y)$ is the wing thickness at the point (x, y) and the integration is over that part of the wing for which the integrand is real.

Equations (5) and (8) show that $F_{0\,W}(x) = A(x)$, the wing transferred area distribution. The alternative expression, equation (9), for $A(x)(= F_{0\,W}(x))$ is due to Ward[2] and suggested writing $F_{nW}(x)$ directly in terms of the wing thickness $T(x, y)$. A form equivalent to equation (9) has been given by Lomax and Heaslet[10].

The wave drag of a thin wing and non-slender body combination will be derived now by using the assumption that the effect on the wave drag of the interference velocity potential, between the exposed wing and the body, is negligible, *i.e.*, the perturbation velocities at infinity are assumed to be given by the body multipoles $F_{n\,B}x)$ and the equivalent wing multipoles $F_{n\,W}(x)$. It follows that the total effective multipole strength function is

$$F_n(x) = F_{n\,B}(x) + F_{n\,W}(x) \qquad \ldots\ \ldots\ \ldots\ \ldots\ \ldots\ \ldots\ \ldots \tag{10}$$

and that the combination wave drag, from equation (7), is

$$D = D\{F_{0\,B} + F_{0\,W}\} + \tfrac{1}{2}\sum_{n=1}^{\infty} D\{F_{2n\,B} + F_{2n\,W}\}\,. \ldots\ \ldots\ \ldots\ \ldots \tag{11}$$

This is the fundamental equation of the present work. Equation (11) enables wave drag estimates to be made using the double integral for $D\{F_{2n\,B} + F_{2n\,W}\}$ given in equation (3), provided that $F_{n\,B}(x)$ and $F_{n\,W}(x)$ are known.

When the fuselage is slender $F_{n\,B}(x) \simeq 0$, $(n > 0)$ and $F_{0\,B}\,(x) = S(x)$ so that equation (11) becomes

$$D = D\{S + F_{0\,W}\} + \tfrac{1}{2}\sum_{n=1}^{\infty} D\{F_{2n\,W}\}$$

which, using $F_{0W}(x) = A(x)$, can be rewritten as

$$D = D\{S + A\} + \tfrac{1}{2}\sum_{n=1}^{\infty} D\{F_{2nW}\}\,.$$

The isolated exposed wing wave drag is

$$D_W = D\{A\} + \tfrac{1}{2}\sum_{n=1}^{\infty} D\{F_{2n\,W}\}$$

and so

$$D = D_W + D\{S + A\} - D\{A\}\,,$$

which is equation (4).

When M tends to 1, from above the special sonic form of equation (11) is obtained. It follows from the work of Lomax and Heaslet[5], for example, that the wave drag is given by $D = D\{F_{0\,B} + F_{0\,W}\}_{M=1}$. This particular result is ' exact ' in the sense that it incorporates no assumptions other than those implied by the use of linearised theory.

An alternative form, which is particularly useful when the wing wave drag is known, is obtained by writing equation (11) in the form

$$D = D_W + D_{WB} + D_B$$

where $D_W = D\{F_{0\,W}\} + \frac{1}{2}\sum_{n=1}^{\infty} D\{F_{2n\,W}\}$ is the isolated exposed wing wave drag

$D_B = D\{F_{0\,B}\} + \frac{1}{2}\sum_{n=1}^{\infty} D\}F_{2n\,B}\}$ is the isolated body wave drag

$$D_{WB} = D\{F_{0\,B} + F_{0\,W}\} - D\{_{0\,B}\} - D\{F_{0\,W}\}$$

$$+ \tfrac{1}{2}\sum_{n=1}^{\infty}\left[D\{F_{2n\,B} + F_{2n\,W}\} - D\{F_{2n\,B}\} - D\{F_{2n\,W}\}\right] \quad .. \quad .. \quad .. \quad (12a)$$

is the interference wave drag. Using the double integral of equation (3) D_{WB} can be written as

$$D_{WB} = -\frac{q}{\pi}\int\int F_{0\,B}''(x_1)F_{0\,W}(x_2)\log|x_1 - x_2|\,dx_1\,dx_2$$

$$-\frac{q}{2\pi}\sum_{n=1}^{\infty}\int\int F_{2n\,B}''(x_1)F_{2n\,W}''(x_2)\log|x_1 - x_2|\,dx_1\,dx_2\,, \quad .. \quad .. \quad .. \quad (12b)$$

which is the generalisation of the result given in equation (6b) for configurations with slender fuselages. It is recommended that the interference wave drag D_{WB} be used in calculations only when one or two fuselage multipoles $F_{n\,B}(x)$ are present, as otherwise the calculations are too complicated.

For completeness, configurations with bodies, such as engine nacelles, mounted on the wing will be discussed very briefly. Provided that these subsidiary bodies are slender, equations (2) and (9) enable the equivalent wing multipole distributions $F_{n\,W}(x)$ to be found by treating the bodies as part of the wing thickness distribution. However, the case when the subsidiary bodies are not slender is much more complex and will not be considered.

3.1.2. *Fuselage Design for Low Wave Drag.*—One of the most important applications of the new wave-drag result, equation (11), lies in the design of fuselages so that the total wave drag is a minimum under certain prescribed conditions. For example, the optimum $F_{n\,B}(x)$ ($n = 0, 2, 4 \ldots$) may be required to give a fuselage of prescribed length and volume and, moreover, they must correspond to a real fuselage shape. It is seen from equation (11) that a number of wave-drag expressions of the form $D\{F_{2n\,B} + F_{2n\,W}\}$ are required to be minimised separately with $F_{2n\,W}(x)$, being a wing term, fixed. Each optimisation problem is of the same type as that discussed in section 2.2 for configurations with slender fuselages and therefore the optimum functions available[9] may be of use.

3.2. *Comparison with the Lomax-Heaslet Multipole Method.*—It is difficult to give a precise definition in general terms of the Lomax-Heaslet multipole method[5] since it has been presented for application to an elliptic wing and body combination. The following comments are based on what is believed to be a correct interpretation of the method. For application to a general configuration an exact method appears to be intended. Thus, in order to determine the wave drag, axial multipole representations are required for the isolated fuselage and for the interference velocity potential. Since the determination of the latter multipole representation usually involves complex calculations, the Lomax-Heaslet method is not simple to apply in either estimation of wave drag or fuselage design for low wave drag. The present multipole method neglects the effect on the wave drag of the interference velocity potential and is not exact; however, it is simpler than the Lomax-Heaslet method and much more readily applicable to the design of fuselages for low total wave drag. Therefore the present method may be preferable in many applications even though it incorporates an assumption.

The Lomax-Heaslet multipole method[5], as applied to the elliptic wing and body combination, is not entirely satisfactory. The wave drag of a so-called unmodified combination, with an axisymmetric fuselage, is determined by neglecting the interference velocity potential between the exposed wing and the body; this is the same assumption as that used throughout the present note. Now, however, the derivation by Lomax and Heaslet of an optimum fuselage shape for low combination wave drag requires careful examination. Lomax and Heaslet take the gross wing, extending through the body, as the basic wing and use the body multipoles to cancel, as completely as possible, the equivalent gross-wing multipoles. This procedure is not satisfactory unless the exposed wing is taken as the basic element. Furthermore, the optimum fuselage is defined as a stream surface of a singularity distribution, so that the singularity representation of the modified configuration is exact. For this reason comparisons between the wave drag of an unmodified combination, deduced using an assumption, and the wave drag of modified combinations, deduced without using any assumptions, are not necessarily valid. Therefore the comparisons of this type that have been given by Lomax and Heaslet[5] are inconsistent.

4. *Discussion of the Fundamental Assumption.*—The assumption fundamental to the present method of estimating wave drag is that the effect on the wave drag of the interference velocity potential, due to the interaction between the exposed wing and the body, is negligible. Here the validity of this assumption is investigated using three known results of supersonic linearised theory for wing-body combinations*.

4.1. *Estimation of Wave Drag.*—Following Nielsen and Pitts[12], consider a circular cylindrical body with a rectangular wing of double-wedge section†. The aspect ratio of the wing is assumed to be high enough for the wing-tip zone of influence not to include the wing-body junction. Fig. 2 shows the wave drag of such a combination as a function of the ratio BR/c, where $B = \sqrt{(M^2 - 1)}$, R is the body radius and c is the wing-root chord.

The present method can be applied to this configuration also by using equation (11) with $F_{2n\,B}(x) = 0$ for all n and gives a wave drag the same as that of the isolated exposed wing. The wave drag of the isolated exposed wing has been determined in Ref. 15, and independently by Lock[14], and the results are plotted in Fig. 2. It should be noted that the fundamental assumption is theoretically exact for $BR/c = 0, \infty$ (i.e., $M = 1, \infty$ for example). This observation can be shown to be true in general[4]. Furthermore, the errors introduced by the assumption are nowhere large. The maximum error is about 7 per cent of the correct wave drag and occurs at $BR/c = 0{\cdot}2$. For this particular combination Fig. 2 shows that the wave drag of the isolated exposed wing is very nearly the same as that of the isolated net wing, which is formed by placing together the panels of the exposed wing.

Since the comparison of Fig. 2 is for rectangular wing-body combinations only, it gives no indication of the errors likely to arise in applications of the present method to general configurations. Experimental evidence or extensive theoretical evidence will be required to extend the comparison of Fig. 2 to a systematic series of wing-body combinations.

Conical wing-body combinations have been investigated by Browne, Friedman and Hodes[15] who present results which are exact within the accuracy of the supersonic linearised theory. It can be shown that the interference velocity potential is very small for their conical combinations, *i.e.*, the fundamental assumption is valid approximately for such special configurations whose interference flow fields are, however, atypical.

---

* Another result has been given by Fraenkel[12] recently. It has been shown that the fundamental assumption is valid when the body is a slender quasi-cylinder of almost circular cross-section.

† Lock[14] has presented an improved method of calculating the wave drag of rectangular wings and quasi-cylindrical body combinations.

4.2. *Design of Quasi-cylindrical Fuselages.*—An important aspect of the present method is the design of fuselages for low combination wave drag. This means that estimates of the wave-drag changes associated with fuselage modifications are to be made. One may ask: how reliable are these estimates ? In the case of quasi-cylindrical fuselages they may be very good. For, it will be seen from Nielsen[6], for example, that the interference velocity potential is invariant with respect to changes in the fuselage, the mean cylinder being fixed (the exposed wing varies with fuselage shape but this variation is unimportant because the fuselage is quasi-cylindrical). Therefore, although the wave-drag estimates of the present method are in error because the interference velocity potential has been neglected, it follows that the present method may predict the correct changes of wave drag when the quasi-cylindrical fuselage only is allowed to vary. It is suggested that the present method can be used to estimate wave-drag changes associated with fuselage modifications with acceptable accuracy, whether the fuselage is a quasi-cylinder or not. Of course, only qualitative estimates would be expected at transonic speeds where the linearised theory is not valid. This important conclusion is supported by the limited experimental evidence available in Ref. 11.

5. *Example—Elliptic Wing and Body Combination.*—Elliptic wing and body combinations have been examined by Lomax and Heaslet[5]. The thickness distribution of the gross elliptic wing is chosen so that all the elemental area distributions, defined by equation (2), represent Sears-Haack bodies (*i.e.*, bodies of given length with minimum wave drag for a given volume). This special wing is discussed by Lomax and Heaslet[5], for example, and was investigated first by Jones[16]. It has a parabolic-arc section with the thickness/chord ratio proportional to local chord.

5.1. *Wave Drag of Exposed Elliptic Wings.*—Before estimating the wave drag of the combination it is necessary to determine the wave drag of the exposed elliptic wing. This may be done by using the result[5] that the wave drag of the exposed elliptic wing is

$$D_W = D_{W0}\left(1 - 2\frac{V_{\Delta W}}{V_{W0}}\right) + D_{\Delta W}\,, \qquad \text{(13)}$$

where D_{W0} is the wave drag of the isolated gross elliptic wing

$D_{\Delta W}$ is the wave drag of the isolated blanketed wing, that is, the portion of the gross wing blanketed by the body

V_{W0} is the volume of the gross elliptic wing

$V_{\Delta W}$ is the volume of the blanketed wing.

The wave drag of the isolated gross elliptic wing may be written[4] as

$$D_{W0} = qt_0{}^2\frac{\pi^3 A_0{}^2}{8}\left(1 + \frac{\pi^2 A_0{}^2 B^2}{32}\right)\Big/\left(1 + \frac{\pi^2 A_0{}^2 B^2}{16}\right)^{3/2}, \qquad \text{(14a)}$$

where q is the kinetic pressure $\frac{1}{2}\rho_0 U^2$

t_0 is the centre-line thickness at the wing mid-chord

A_0 is the aspect ratio

$B = \sqrt{(M^2 - 1)}$.

The volume of the wing is

$$V_{W0} = c_0{}^2 t_0 \frac{\pi^2 A_0}{32}\,, \qquad \text{(14b)}$$

where c_0 is the maximum wing chord. An alternative expression for the wave drag can be obtained using equation (9) together with the result

$$D_{W0} = D\left\{F_{0\,W0}\right\} + \tfrac{1}{2}\sum_{n=1}^{\infty} D\left\{F_{2n\,W0}\right\},$$

i.e., D_{W0} has been expressed in terms of the wave drags associated with the elliptic wing's equivalent multipole strength functions $F_{n\,W0}(x)$. The wave drags associated with the first three non-zero multipole strength functions $F_{0\,W0}(x)$, $F_{2\,W0}(x)$ and $F_{4\,W0}(x)$ have been calculated by Lomax and Heaslet[5], whose results are given in Fig. 3. It will be seen that the wave drag associated with the higher order multipoles becomes a large proportion of D_{W0} only for values of A_0B that are not small. When $A_0B = 0$ (i.e., $M = 1$), only the one multipole strength function $\left[F_{0\,W0}(x)\right]_{M=1}$ is required. This means that the wing is 'slender', in the aerodynamic sense, and so its wave drag depends solely upon the distribution of cross-sectional area.

The wave drag of the isolated blanketed elliptic wing, $D_{\Delta W}$, cannot be determined simply without introducing a further approximation. Two such approximations are to treat the blanketed wing as slender[4] or as a rectangular wing[5]. The former approximation is more useful near $M = 1$, while the latter is preferable at higher Mach numbers. The rectangular wing approximation, introduced by Lomax and Heaslet[5], will be used here. This equivalent rectangular wing will have a chord c_0, thickness along mid-chord t_0 and a span d equal to the diameter of the body enclosing it. With this approximation the wave drag of the blanketed wing is[17]

$$D_{\Delta W} = \frac{q\left(\frac{d}{c_0}\right)t_0^{\,2}}{B} \times \begin{cases} \dfrac{16}{\pi} B\left(\dfrac{d}{c_0}\right)\left[\dfrac{\sin^{-1} B\left(\dfrac{d}{c_0}\right)}{B\left(\dfrac{d}{c_0}\right)} - \tfrac{1}{6}\sqrt{\left\{1 - B^2\left(\dfrac{d}{c_0}\right)^2\right\}} + \left(1 - \dfrac{B^2\left(\dfrac{d}{c_0}\right)^2}{6}\right)\cosh^{-1}\left(\dfrac{1}{B\left(\dfrac{d}{c_0}\right)}\right)\right], & B\left(\dfrac{d}{c_0}\right) \leqslant 1, \\ \dfrac{16}{3}, & B\left(\dfrac{d}{c_0}\right) \geqslant 1. \end{cases} \quad \ldots \quad \ldots \quad (15a)$$

The ratio (d/c_0) is the aspect ratio of the equivalent rectangular wing. The volume is given by

$$V_{\Delta W} = \tfrac{2}{3} d c_0 t_0 . \quad \ldots \quad \ldots \quad \ldots \quad \ldots \quad \ldots \quad \ldots \quad \ldots \quad \ldots \quad \ldots \quad \ldots \quad (15b)$$

Equations (14b), (15b) enable the wave drag of the exposed elliptic wing, given by equation (13), to be written in the approximate form

$$D_W = D_{W0}\left(1 - \frac{16}{3\pi}\left(\frac{d}{b}\right)\right) + D_{\Delta W}, \quad \ldots \quad \ldots \quad \ldots \quad \ldots \quad \ldots \quad \ldots \quad \ldots \quad (16)$$

where D_{W0} and $D_{\Delta W}$ are given by equations (14a), (15a) respectively.

5.2. *Wave Drag of the Combination.*—The wave drag of a wing-body combination, given by equation (11), may be written in the form

$$D = D_W + D\left\{F_{0\,B} + F_{0\,W}\right\} - D\left\{F_{0\,W}\right\} + \tfrac{1}{2}\sum_{n=1}^{\infty}\left[D\left\{F_{2n\,B} + F_{2n\,W}\right\} - D\left\{F_{2n\,W}\right\}\right].$$

For the special case when the fuselage multipole representation is such that $F_{n\,B}(x) = 0$, $n > 2$ this result becomes

$$D = D_W + D\{F_{0\,B} + F_{0\,W}\} - D\{F_{0\,W}\} + \tfrac{1}{2}[D\{F_{2\,B} + F_{2\,W}\} - D\{F_{2\,W}\}] . \quad .. \quad (17)$$

Equation (17) shows that the minimum wave drag, obtained by using the fuselage quadrupole distribution $F_{2\,B}(x)$, occurs when $F_{2\,B}(x) = -F_{2\,W}(x)$. This minimum may, however, not be realised in practice because $F_{2\,B}(x)$ must correspond to a realistic fuselage shape.

It is interesting to compare equation (17) with equation (4) which is applicable to combinations incorporating slender fuselages. Although $F_{0\,W}(x)$ is equal to the transferred area distribution $A(x)$, it does not follow that $F_{0\,B}(x)$ is equal to the fuselage cross-sectional area distribution $S(x)$. Nevertheless, a useful approximation for nearly-slender fuselages is to replace $F_{0B}(x)$ by $S(x)$. The wave drag of the elliptic wing-body combination may now be written in the approximate form

$$D = D_W + D\{S + A\} - D\{A\} + \tfrac{1}{2}[D\{F_{2\,B} + F_{2\,W}\} - D\{F_{2\,W}\}] , \quad .. \quad .. \quad (18)$$

where D_W, the wave drag of the exposed elliptic wing, is given by equation (16).

Equation (18) can be used to estimate the minimum possible wave drag for the case when, for example, only the fuselage length, volume and base area are specified but the wing is fixed. Assuming that the fuselage shape corresponding to $F_{2\,B}(x) = -F_{2\,W}(x)$ is not unrealistic, the minimum wave drag is given by

$$D_{\min} = D_W + D_{\min}\{S + A\} - D\{A\} - \tfrac{1}{2}D\{F_{2\,W}\} ,$$

where $D_{\min}\{S + A\}$ denotes the wave drag associated with a so-called optimum area distribution appropriate to the constraints on the fuselage cross-sectional area distribution $S(x)$. Now, Fig. 3 gives the wave drags associated with the first three non-zero gross wing equivalent multipoles. If these results were available for the exposed wing also then the total wave drag could be found. However, since they are not available some results will be found by assuming that

$$D\left\{F_{n\,W}\right\} = \frac{D_W}{D_{W0}} D\left\{F_{n\,W0}\right\} , \qquad n = 0, 2, 4, \ldots ,$$

where D_{W0} is the wave drag of the gross elliptic wing and $F_{n\,W0}(x)$ ($n = 0, 2, 4, \ldots$) defines the gross wing equivalent multipole distributions. It is worthy of note that this approximation is compatible with the relation $D_W = D\left\{F_{0\,W}\right\} + \frac{1}{2}\sum_{n=1}^{\infty} D\left\{F_{2n\,W}\right\}$. The minimum wave drag becomes

$$D_{\min} = D_W + D_{\min}\{S + A\} - \frac{D_W}{D_{W0}}\left[D\left\{F_{0\,W0}\right\} + \tfrac{1}{2}D\left\{F_{2\,W0}\right\}\right] . \quad .. \quad .. \quad (19)$$

Here D_W, D_{W0} are given by equations (14a), (15a), (16) and $D\{F_{0\,W0}\}$, $D\{F_{2\,W0}\}$ are to be found from Fig. 3.

The predictions of equation (19) may have only a qualitative significance because the additional approximation

$$D\left\{F_{n\,W}\right\} = \frac{D_W}{D_{W0}} D\left\{F_{n\,W0}\right\}$$

has been made. Nevertheless, numerical results with a quantitative significance can be obtained provided that this approximation is not used; then it is necessary to calculate each required multipole distribution $F_{n\,W}(x)$ for the exposed wing before calculating its associated wave drag (from equations (3) and (9)).

5.3. *Comparison with Experiment.*—It is not possible to compare with experiment the predictions of equation (18), which gives the wave drag of the elliptic-wing–body combination, except for the special case when the fuselage is axisymmetric (i.e., $F_{2B}(x) = 0$) and $S(x)$ is a so-called optimum area distribution, whose associated wave drag is a minimum for given length, volume and base area. This case has been investigated by Lomax and Heaslet[5], whose theoretical result for the wave drag of this elliptic-wing–unmodified-body combination is the same as that deduced from equation (18).

Fig. 4 compares the theoretical and experimental wave drag for this configuration. The theoretical result can be reduced to the form $C_D = C_{DW} + 0{\cdot}0054$, the wave-drag coefficients being based on the gross wing area. Lomax and Heaslet[5] point out that the quantitative agreement for the total wave drag, less the isolated fuselage wave drag, is very good for $M > 1{\cdot}15$. Thus the present method, which neglects the interference velocity potential between the exposed wing and the fuselage, has predicted the interference wave drag with remarkable accuracy.

The configuration denoted as modified by Lomax and Heaslet[5] has a fuselage which is not axisymmetric. However, the isolated fuselage multipole representation is not known because the fuselage has been defined as a stream surface of the singularity distribution representing the entire configuration. Therefore the effect of fuselage quadrupoles cannot be examined without further experimental data. The theoretical minimum wave drag in this case is given approximately by equation (19) and is shown in Fig. 4, which illustrates the importance of fuselage quadrupoles in reducing the wave drag of a wing-body combination. The minimum wave drag when the fuselage is axisymmetric is shown also. These results show that, theoretically, the usefulness of the multipole method as a means of reducing the wave drag does not decrease with increasing Mach number. On the other hand, it appears from the calculations of Lomax and Heaslet[5] that the optimum quadrupole strength defined by $F_{2B}(x) = -F_{2W}(x)$ may not be usable at the higher Mach numbers; unrealistic fuselages with surface streamlines crossing each other may be obtained if $F_{2B}(x)$ is chosen to be equal to $-F_{2W}(x)$. Finally, it must be emphasised that the two lower curves in Fig. 4 do not represent the wave-drag variation with Mach number for a certain configuration but only the minimum wave drag possible for an optimum design at a specific Mach number.

6. *Conclusion.*—The Lomax-Heaslet special multipole method for estimating the wave drag of combinations of thin wings and non-slender bodies has been examined and what is believed to be an improved method presented. The inconsistencies that arose in applications of the Lomax-Heaslet multipole method have been eliminated by using the assumption that the effect on the wave drag of the interference velocity potential, due to the interaction between the exposed wing and the body, is negligible. Since this assumption is fundamental to the area-rule method of wave-drag estimation it has provided a very satisfactory basis for an extension of the area rule to combinations incorporating fuselages that are not slender. The extension described in this paper is applicable to problems involving both estimation of wave drag and design for low combination wave drag.

The accuracy of the predictions of the present method has been examined in a number of special cases. Theoretically, a comparison has been made with existing results for rectangular wing–circular cylindrical body combinations; in addition, a brief investigation of conical configurations and combinations employing quasi-cylindrical fuselages has been made. Experimentally, a comparison has been made for the wave drag of an elliptic wing and axisymmetric body combination. These comparisons with theory and experiment enable two important conclusions to be made. Firstly, estimates of the wave-drag changes associated with changes in fuselage shape are likely to have a quantitative significance. Secondly, estimates of total combination wave drag may have a quantitative or only a qualitative significance; quantitative agreement would not be expected at transonic speeds where the supersonic linearised theory is not valid.

NOTATION

$a_n(x)$		Usual nth order multipole strength function
A_0		Gross wing aspect ratio
$A(x)$		Transferred area distribution of exposed wing
$A_n(x)$		Alternative nth order multipole strength function (*see* equation (A.1))
b		Total wing span
B	$=$	$\sqrt{(M^2-1)}$
c		Wing chord
c_0		Gross wing-root chord
C_D		Wave-drag coefficient, based on an appropriate area
d		Diameter of body enclosing blanketed wing
D		Total wave drag
D_W		Isolated exposed wing wave drag
D_{WB}		Interference wave drag
B_B		Isolated body wave drag
$D\{S\}$		Wave drag associated with the ' area ' distribution $S(x)$ (*see* equation (3))
$F_n(x)$		Modified nth order multipole strength function (*see* equation (A.5))
$F_{nB}(x)$		Modified nth order fuselage multipole strength function
$F_{nW}(x)$		Effective modified nth order multipole strength function of the exposed wing
l		Fuselage length
M		Free-stream Mach number
q		Kinetic pressure $\frac{1}{2}\rho_0 U_0^2$
r		Cylindrical polar co-ordinate (*see* Fig. 1)
R		Radius (of cylindrical body)
$S(x)$		Fuselage cross-sectional area distribution
$S(x, \theta, M)$		Elemental area distribution
$S_W(x, \theta, M)$		Exposed wing elemental area distribution (*see* equation (2))
t_0		Root thickness at wing mid-chord
$T(x, y)$		Wing thickness at the point $(x, y, 0)$
U_0		Free-stream velocity
V		Volume
(x, s, θ)		Cylindrical polar co-ordinates (*see* Fig. 1)
(x, y, z)		Rectangular Cartesian co-ordinates (*see* Fig. 1)
θ		Cylindrical polar co-ordinate (*see* Fig. 1)
ρ_0		Free-stream density

NOTATION—*continued*

$\phi(x, r, \theta)$	Perturbation velocity potential (the velocity component in the free stream direction is defined to be $U_0 + \dfrac{\partial \phi(x, r, \theta)}{\partial x}$)
$_{1, 2}$	Subscripts denoting integration variable, e.g., x_1, x_2
Dashes	Denote partial differentiation with respect to x, e.g., $S'(x, \theta, M) = \dfrac{\partial S(x, \theta, M)}{dx}$
$_{x, r, \theta}$	Subscripts denoting partial differentiation, e.g., $\phi_r = \partial\phi/\partial r$
$_{B, W, W0, WN, \Delta W}$	Subscripts denoting fuselage (or body), exposed wing, gross wing, net wing, blanketed wing respectively, e.g., V_{W0} denotes the volume of the gross wing
$_n$	Integer subscript for functions defining the nth order multipole distribution $_{n=0, 1, 2, \ldots}$
$_{\min}$	Denotes a minimum value, e.g., $D_{\min}$ is the minimum wave drag

---

REFERENCES

No.	*Author*	*Title, etc.*
1	R. T. Jones	Theory of wing-body drag at supersonic speeds. N.A.C.A. Research Memo. A53H18a (TIB/3890). September, 1953.
2	G. N. Ward	The drag of source distributions in linearised supersonic flow. College of Aeronautics Report 88. A.R.C. 17,478. February, 1955. (Also A.R.C. 17,836 (Unpublished).)
3	B. S. Baldwin and R. R. Dickey ..	Application of wing–body theory to drag reduction at low supersonic speeds. N.A.C.A. Research Memo. A54J19 (TIB/4534). January, 1955.
4	L. M. Sheppard	Methods for determining the wave drag of non-lifting wing–body combinations. R.A.E. Report Aero. 2590. A.R.C. 19,320. April, 1957.
5	H. Lomax and M. A. Heaslet ..	A special method for finding body distortions that reduce the wave drag of wing and body combinations at supersonic speeds. N.A.C.A. Research Memo. A55B16 (TIB/4679). May, 1955.
6	J. N. Nielsen	General theory of wave drag reduction for combinations employing quasi-cylindrical bodies with an application to swept wing and body combinations. N.A.C.A. Research Memo. A55B07 (TIB/4712). June, 1955.
7	R. C. Lock	A note on the application of the supersonic area rule to the determination of the wave drag of rectangular wings. *J. Fluid Mech.* Vol. II. Part 6. August, 1957.
8	E. Eminton	On the minimisation and numerical evaluation of wave drag. R.A.E. Report Aero. 2564. A.R.C. 19,212. November, 1955.
9	C. Ferrari	Determination of the external contour of a body of revolution with a central duct so as to give minimum drag in supersonic flow with various perimetral conditions imposed upon the missile geometry. Cornell Aero. Lab. Report AF–814–A–1. March, 1953.

REFERENCES—*continued*

No.	*Author*	*Title, etc.*
10	H. Lomax and M. A. Heaslet ..	Recent developments in the theory of wing–body wave drag. *J.Ae.Sci.* Vol. 23. No. 12. December, 1956.
11	L. E. Fraenkel	The wave drag of wing-quasi-cylinder combinations at zero incidence. Imperial College Department of Aeronautics Paper No. 41. 1956.
12	J. N. Nielsen and W. C. Pitts ..	Wing–body interference at supersonic speeds with an application to combinations with rectangular wings. N.A.C.A. Tech. Note 2677. April, 1952.
13	R. C. Lock	An extension of the linearised theory of supersonic flow past quasi-cylindrical bodies, with application to wing–body interference. A.R.C. 19,112. March, 1957. (To be published.)
14	L. M. Sheppard	A note on the wave drag of the wing of a rectangular wing and body combination. R.A.E. Tech. Note Aero. 2494. A.R.C. 19,318. February, 1957.
15	S. H. Browne, L. Friedman and I. Hodes	A wing–body problem in a supersonic conical flow. *J. Ae. Sci.* Vol. 15. No. 8. August, 1948.
16	R. T. Jones	Theoretical determination of the minimum drag of airfoils at supersonic speeds. *J. Ae. Sci.* Vol. 19. No. 12. December, 1952.
17	S. M. Harmon	Theoretical supersonic wave drag of untapered swept-back and rectangular wings at zero lift. N.A.C.A. Tech. Note 1449. October, 1947.
18	R. H. Cramer	Interference between wing and body at supersonic speeds—Theoretical and experimental determination of pressures on the body. *J. Ae. Sci.* Vol. 18. No. 9. September, 1951.

APPENDIX

Properties of Axial Multipole Distributions

Distributions of non-lifting multipole singularities along the line $y = 0$, $z = 0$, which is parallel to the free-stream direction (*see* Fig. 1), will be considered in the Appendix. The perturbation velocity potential ϕ, due to such a distribution of multipoles, may be written in the form

$$\phi(x, r, \theta) = -\frac{1}{2\pi}\sum_{n=0}^{\infty}\cos n\theta \int_0^{x-Br} \frac{A_n(x_1)\cosh\left[n\cosh^{-1}\left(\frac{x-x_1}{Br}\right)\right]dx_1}{\sqrt{\{(x-x_1)^2 - B^2r^2\}}}, \quad .. \quad .. \quad (A.1)$$

where (x, r, θ) are cylindrical polar co-ordinates (*see* Fig. 1),

$A_n(x)$ is a multipole strength function defining the nth order multipole distribution ($n = 0, 1, 2, \ldots$)

and the nth order multipoles are defined for $x \geqslant 0$, so that $\phi(x, r, \theta)$ is identically zero for $x \leqslant Br$. It is assumed that $A_n(x)$ is continuous everywhere, *i.e.*, each multipole distribution is ' smooth '. The particular form of equation (A.1) is due to Cramer[18] and has been given by Lomax and Heaslet[5]. A more usual form of equation (A.1) is

$$\phi(x, r, \theta) = -\frac{1}{2\pi}\sum_{n=0}^{\infty} r^n \cos n\theta \left(\frac{1}{r}\frac{\partial}{\partial r}\right)^n \int_0^{x-Br} \frac{a^n(x_1)\,d_1}{\sqrt{\{(x-x_1)^2 - B^2r^2\}}},$$

where the strength function $a_n(x)$ is related to $A_n(x)$ in equation (A.1) by the result[5]

$$(-B)^n \frac{\partial^n a_n(x)}{\partial x^n} = A_n(x).$$

Since an nth order multipole can be considered to consist of 2^n poles (or sources) a source is a *zero*th-order multipole, a doublet is a first-order multipole and a quadrupole is a second-order multipole.

If any streamtube of a multipole distribution is symmetrical about the plane $y = 0$ (*see* Fig. 1), then the strength functions $A_n(x)$, $a_n(x)$ are identically zero for odd values of n. This symmetry condition will be satisfied by the configurations examined in this note; thus only the even multipoles are considered.

From equation (A.1) it may be shown[5] that the perturbation velocities associated with an axial multipole distribution are

$$\phi_x(x, r, \theta) = -\frac{1}{2\pi}\sum_{n=0}^{\infty}\cos n\theta \int_0^{x-Br} \frac{A_n'(x_1)\cosh\left[n\cosh^{-1}\left(\frac{x-x_1}{Br}\right)\right]dx_1}{\sqrt{\{(x-x_1)^2 - B^2r^2\}}} \quad .. \quad .. \quad \text{(A.2)}$$

$$\frac{1}{r}\phi_\theta(x, r, \theta) = \frac{1}{2\pi r}\sum_{n=0}^{\infty} n\sin n\theta \int_0^{x-Br} \frac{A_n(x_1)\cosh\left[n\cosh^{-1}\left(\frac{x-x_1}{Br}\right)\right]dx_1}{\sqrt{\{(x-x_1)^2 - B^2r^2\}}} \quad .. \quad .. \quad \text{(A.3)}$$

and

$$\phi_r(x, r, \theta) = \frac{1}{2\pi}\int_0^{x-Br} \frac{(x-x_1)A_0'(x_1)\,dx_1}{r\sqrt{\{(x-x_1)^2 - B^2r^2\}}}$$

$$+ \frac{B}{4\pi}\sum_{n=1}^{\infty}\cos n\theta \int_0^{x-Br} \frac{A_n'(x_1)\left\{\begin{array}{l}\cosh\left[(n+1)\cosh^{-1}\left(\frac{x-x_1}{Br}\right)\right] \\ +\cosh\left[(n-1)\cosh^{-1}\left(\frac{x-x_1}{Br}\right)\right]\end{array}\right\}dx_1}{\sqrt{\{(x-x_1)^2 - B^2r^2\}}}, \quad \text{(A.4)}$$

where $A_n'(x)$ denotes $\partial A_n/\partial x$ and the suffix notation for partial differentiation is used. The contribution of any $A_n(x)$ to a perturbation velocity potential is zero for $x \leqslant Br$, where $\phi(x, r, \theta)$ is identically zero.

The wave drag associated with a smooth axial multipole distribution has been found by, among others, Lomax and Heaslet[5] who used a control-surface method of calculation. The perturbation velocities on an infinite circular cylindrical control surface were determined using equations (A.2), (A.3), (A.4). Let a new multipole strength function $F_n(x)$ be defined by

$$A_n(x) = U_0 F_n'(x) \quad .. \quad .. \quad .. \quad .. \quad .. \quad .. \quad .. \quad .. \quad .. \quad \text{(A.5)}$$

Then the wave drag[5] may be written as

$$D = D\{F_0\} + \tfrac{1}{2}\sum_{n=1}^{\infty} D\{F_n\}, \quad .. \quad .. \quad .. \quad .. \quad .. \quad .. \quad .. \quad \text{(A.6)}$$

where $D\{F_n\}$ is given by equation (3) and defines the wave drag associated with $F_n(x)$. It should be noted that each $F_n'(x)$ is continuous everywhere because the multipole distributions are smooth.

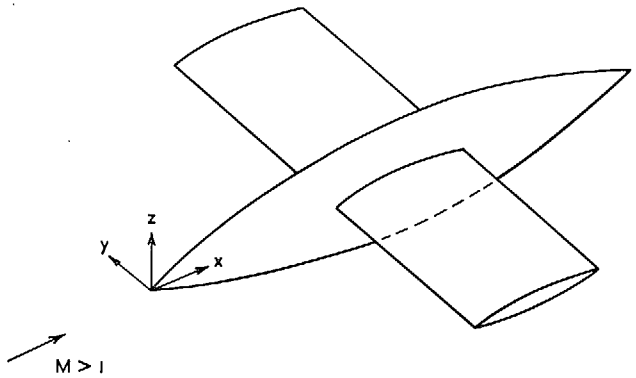

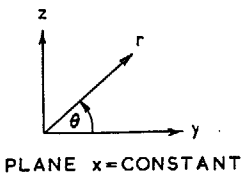

FIG. 1. Co-ordinate system for wing–body combination.

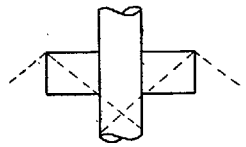

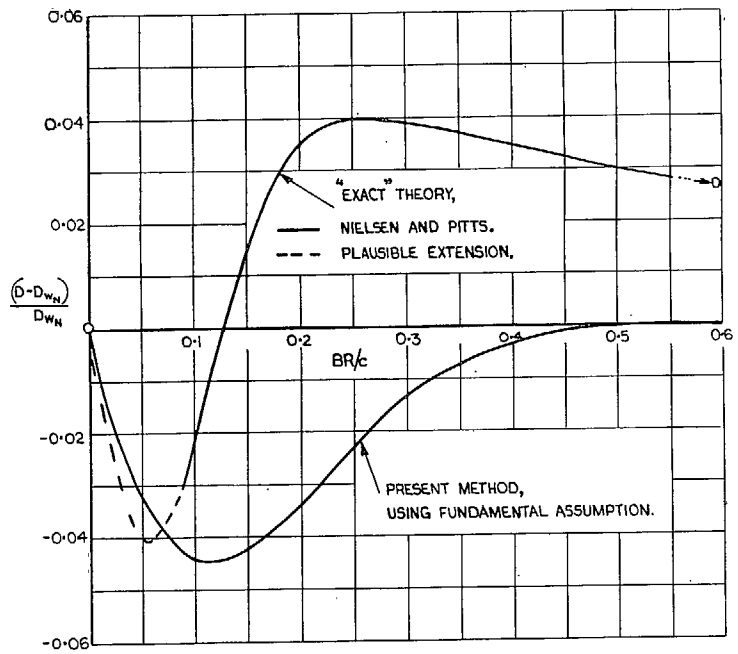

FIG. 2. Wave drag, D, of a rectangular wing of double-wedge section mounted on a circular cylindrical body $(B(b - d)/c = 2)$.

(71665) Wt. 52/8943 K.7 2/58 Hw.

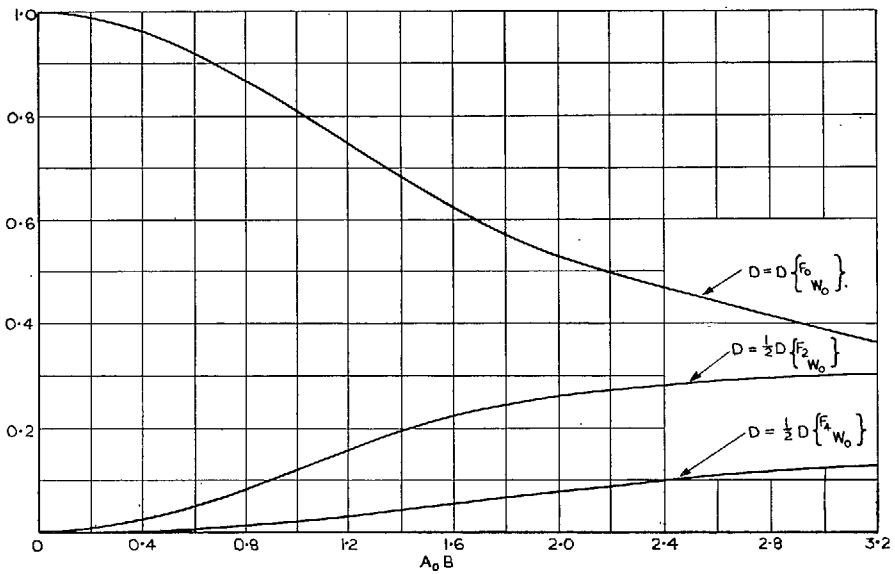

FIG. 3. Portions of gross elliptic wing wave drag associated with the equivalent multipole distributions $F_{\pi W0}(x)$ $(n = 0, 2, 4)$.

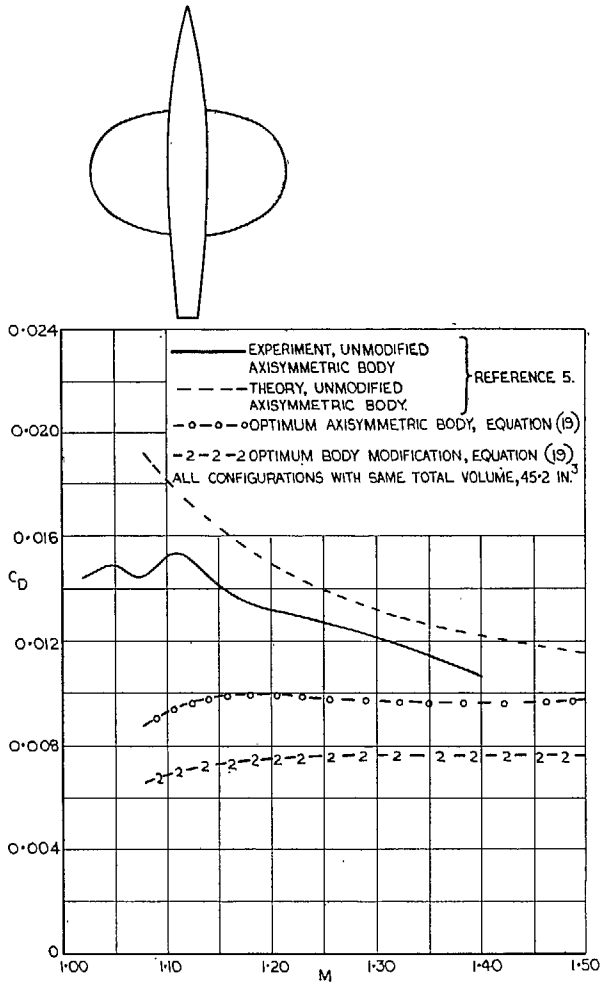

WAVE DRAG COEFFICIENT BASED ON THE GROSS WING AREA, 40·5 IN.²
BODY : LENGTH = 21 IN., V_B = 41·90 IN.³, BASE AREA = 1·23 IN.²
WING : β = 11·02 IN., C_0 = 4·68 IN., t_0 = 0·234 IN., A_0 = 3,
V_{W_0} = 4·74 IN.³, V_W = 3·32 IN.³
MIDCHORD OF WING IS SITUATED 11·47 IN. DOWNSTREAM OF BODY NOSE; AT THIS POSITION UNMODIFIED BODY RADIUS IS 1·01 IN.

FIG. 4. Theoretical and experimental results for the wave drag of an elliptic-wing–body combination.

PRINTED IN GREAT BRITAIN

Publications of the Aeronautical Research Council

ANNUAL TECHNICAL REPORTS OF THE AERONAUTICAL RESEARCH COUNCIL (BOUND VOLUMES)

1939 Vol. I. Aerodynamics General, Performance, Airscrews, Engines. 50*s.* (52*s.*).
Vol. II. Stability and Control, Flutter and Vibration, Instruments, Structures, Seaplanes, etc. 63*s.* (65*s.*)

1940 Aero and Hydrodynamics, Aerofoils, Airscrews, Engines, Flutter, Icing, Stability and Control, Structures, and a miscellaneous section. 50*s.* (52*s.*)

1941 Aero and Hydrodynamics, Aerofoils, Airscrews, Engines, Flutter, Stability and Control, Structures. 63*s.* (65*s.*)

1942 Vol. I. Aero and Hydrodynamics, Aerofoils, Airscrews, Engines. 75*s.* (77*s.*)
Vol. II. Noise, Parachutes, Stability and Control, Structures, Vibration, Wind Tunnels. 47*s.* 6*d.* (49*s.* 6*d.*)

1943 Vol. I. Aerodynamics, Aerofoils, Airscrews. 80*s.* (82*s.*)
Vol. II. Engines, Flutter, Materials, Parachutes, Performance, Stability and Control, Structures. 90*s.* (92*s.* 9*d.*)

1944 Vol. I. Aero and Hydrodynamics, Aerofoils, Aircraft, Airscrews, Controls. 84*s.* (86*s.* 6*d.*)
Vol. II. Flutter and Vibration, Materials, Miscellaneous, Navigation, Parachutes, Performance, Plates and Panels, Stability, Structures, Test Equipment, Wind Tunnels. 84*s.* (86*s.* 6*d.*)

1945 Vol. I. Aero and Hydrodynamics, Aerofoils. 130*s.* (132*s.* 9*d.*)
Vol. II. Aircraft, Airscrews, Controls. 130*s.* (132*s.* 9*d.*)
Vol. III. Flutter and Vibration, Instruments, Miscellaneous, Parachutes, Plates and Panels, Propulsion. 130*s.* (132*s.* 6*d.*)
Vol. IV. Stability, Structures, Wind Tunnels, Wind Tunnel Technique. 130*s.* (132*s.* 6*d.*)

Annual Reports of the Aeronautical Research Council—

1937 2*s.* (2*s.* 2*d.*) 1938 1*s.* 6*d.* (1*s.* 8*d.*) 1939–48 3*s.* (3*s.* 5*d.*)

Index to all Reports and Memoranda published in the Annual Technical Reports, and separately—

April, 1950 - - - - R. & M. 2600 2*s.* 6*d.* (2*s.* 10*d.*)

Author Index to all Reports and Memoranda of the Aeronautical Research Council—

1909—January, 1954 R. & M. No. 2570 15*s.* (15*s.* 8*d.*)

Indexes to the Technical Reports of the Aeronautical Research Council—

December 1, 1936—June 30, 1939	R. & M. No. 1850	1*s.* 3*d.* (1*s.* 5*d.*)
July 1, 1939—June 30, 1945	R. & M. No. 1950	1*s.* (1*s.* 2*d.*)
July 1, 1945—June 30, 1946	R. & M. No. 2050	1*s.* (1*s.* 2*d.*)
July 1, 1946—December 31, 1946	R. & M. No. 2150	1*s.* 3*d.* (1*s.* 5*d.*)
January 1, 1947—June 30, 1947	R. & M. No. 2250	1*s.* 3*d.* (1*s.* 5*d.*)

Published Reports and Memoranda of the Aeronautical Research Council—

Between Nos. 2251–2349	R. & M. No. 2350	1*s.* 9*d.* (1*s.* 11*d.*)
Between Nos. 2351–2449	R. & M. No. 2450	2*s.* (2*s.* 2*d.*)
Between Nos. 2451–2549	R. & M. No. 2550	2*s.* 6*d.* (2*s.* 10*d.*)
Between Nos. 2551–2649	R. & M. No. 2650	2*s.* 6*d.* (2*s.* 10*d.*)
Between Nos. 2651–2749	R. & M. No. 2750	2*s.* 6*d.* (2*s.* 10*d.*)

Prices in brackets include postage

HER MAJESTY'S STATIONERY OFFICE

York House, Kingsway, London W.C.2; 423 Oxford Street, London W.1; 13a Castle Street, Edinburgh 2; 39 King Street, Manchester 2; 2 Edmund Street, Birmingham 3; 109 St. Mary Street, Cardiff; Tower Lane, Bristol 1; 80 Chichester Street, Belfast, *or through any bookseller.*

S.O. Code No. 23-3076